College of Basic Education Researchers Journal. ISSN: 7452-1992 *Vol. (19), No.(4), (2023)*

Influence of the Delay Time on Dynamical Regimes of the Optoelectronics Oscillator Based Mach-Zehnder Modulator MZM with Optoelectronic Feedback

Layla Omar Babarasul
Department of Elementary Sciences, College of Education, University of Garmiyan

Younis Thanoon Younis
Department of Physics College of Education for Pure Sciences University of Mosul

(Received in 29/12/2022 Accepted in 9/3/2023)

Abstract

In this research, we demonstrated the Modeling and simulation of Mach-Zehnder modulator(MZM) with optoelectronic feedback(OEFB) to generate optical instabilities output (periodic, quasi-periodic and chaos spatial signal). The Integrodifferential equation is the basis of this model. Control of the instabilities region of optical output from MZM been done optoelectronic feedback OEF delay time. The results of the numerical solutions of the system of delay differential equations (DDE) for the OEO system showed that there is very large diversity in the oscillation systems, ranging from single oscillation, double-period oscillation, multi-period oscillations, and chaotic oscillations respectively, as functions of the photoelectric feedback delay times τ_D when the linear gain coefficient is fixed at the value of 3. The results of the numerical solutions also showed an increase in the dimensions of the chaotic oscillations at the large values of the delay times τ_D of the optoelectronic feedback. Numerical simulation results of the bifurcation diagram showed wide diversity of oscillation regimes, ranging fromsingle period, period two, mixed-mode, quasi-periodic and chaotic oscillations, which are all functions of delay time parameter τ_D .

Keywords: Optoelectronic feedback, Optoelectronic oscillator, chaos control, and Mach-Zehnder Modulator.

تأثير وقت التأخير على الأنظمة الديناميكية لمذبذب الإلكترونيات الضوئية المعتمد مع ردود الفعل الإلكترونية Mach-Zehnder Modulator MZM على الضوئية

ليال عمر بابارسول

قسم العلوم الابتدائية، كلية التربية، جامعة كرميان

يونس ذنون يونس

قسم الفيزياء كلية التربية للعلوم الصرفة جامعة الموصل

الملخص:

في هذا البحث، أظهرنا نمذجة ومحاكاة لمنظومة مذبذب كهروضوئي يتألف من مضمن ماخ-زيندرMZM مع التغذية الراجعة الكهروضوئية OEFB لتوليد ناتج عدم استقرار بصري (على شكل اشارة راديوية RF ذات احادية الدورة وذات دورات مضاعفة وشبه دورية وفوضى). المعادلة التكاملية التفاضلية هي أساس هذا النموذج. تم التحكم في منطقة عدم الاستقرار للإخراج البصري من المضمن MZM عن طريق وقت تأخيرτ_D للتغذية الراجعة الإلكترونية. أظهرت نتائج الحلول الرقمية لنظام المعادلات التفاضلية المتأخرة DDE لنظام OEO أن هناك تنوعًا كبيرًا جدًا في أنظمة التذبذب للاشارة الراديوية المتولدة بدءًا من التذبذب الفردي والتذبذب المزدوج الدورة والتذبذبات متعددة الفترات والتذبذبات الفوضوية على التوالي ، كوظائف لأوقات تأخير التغذية الكهروضوئية τD. عندما يكون معامل الكسب الخطي ثابتًا بقيمة ٣. وأظهرت نتائج الحلول العددية أيضًا زيادة في أبعاد التذبذبات الفوضوية عند القيم الكبيرة لأوقات التأخير τD لمنظومة التغذية الكهروضوئية الراجعة OEFB. أظهرت نتائج الحلول العددية من خلال مخطط التشعب ان هناك مناطق تذبذب متنوعة جدا تراوحت بين التذبذب المنفرد والتذبذب المضاعف وتذبذبات النمط الممتزج للتذبذبات البطيئة والسريعة وتذبذبات الشبه الدورية وتذبذبات الفوضى وكلها يمكن التحكم بها وتغييرها من خلال متغير التحكم Control parameter والتي في هذه الحالة هي زمن التغذيةالكهروضوئية الراجعة τD.

1- Introduction:

Over the years, a variety of external optical intensity modulators for optical fiber communication applications have been created. Among them, the Mach-Zehnder modulator made of lithium niobate (LiNbO3) is still regarded as having the highest performance. The high optical power handling capacity, wide optical bandwidth, zero or tunable chirp, and low optical loss are the most notable benefits [1]. In the control community, time delay systems are now more significant. Delays happen as a result of processing delays that cause memory effects or finite signal propagation velocities, or, more commonly, infinite-dimensional systems. Delay differential equations can be used to model time delay systems, which frequently have significant nonlinear effects. The theme

of the issue, "Nonlinear Dynamics of Delay Systems," is introduced in this overview article [2,3]. Ikeda-Model the earliest model of the nonlinear system, that proposed ring cavity laser and showed that The transmitted light from a ring cavity containing a uniformly expanded two-level absorber exhibits a multiple-valued response to a continuous incident light while the system is stationary [4].

The optoelectronic oscillator (OEO), which is based on delay time nonlinearities, is one of the most effective devices for producing optical chaotic signals. It works by returning part of the electrical signal (which is detected from optical output after delayed time by optical fiber acting as a delay line of the system) and feeding it back into modulation input term of the electro-optical modulator. Such kind of systems exhibits various kinds of instabilities, such as instability, periodic oscillation [5]. The Ikeda variable of this model is the voltage of the renewing RF signal, which is indicated by Vosc(t), It rotates in a clockwise motion and is the four components of the feedback loop. The nonlinear electrical-to-optical (E/O) and optical-to-electrical (O/E) unit is the initial component. It quantitatively illustrates the nonlinear relationship between the voltage of the RF drive signal for the resonant EO comb generator and the output RF voltage of the photodetector. The second is a fiber delay line, which shows how long an optical signal takes to arrive after traveling through a fiber. The RF amplifier, which describes the RF gain of the feedback RF signal, is the third component, then the signal is filtered by the linear bandpass $\tilde{H}\,BF$ before feeding into RF input port. The signal $V_{osc}(t)$ modulates the optical insertion to MZM, which in turn detected (after flying back through fiber delay line) by photodetector, mathematically represented *as* $f_{NL}(V_{osc}(t\text{-}T))$, then become g. $fNL(V_{osc}(t\text{-}T))$ after amplified by g times by RF amplifier, then the RF signal voltage passes to the bandpass filter and again as input RF modulating signal of MZM. The mentioned scenario is called Ikeda-like OEO closed-loop model, which has four components in the feedback

loop, is depicted in block diagram form in Figure (1) for the time domain model, such that they satisfy the interrelated as:

$$\widehat{M}\{x(t)\} = \beta f_{NL}(x(t-\tau_D)) \qquad \ldots\ldots (1)$$

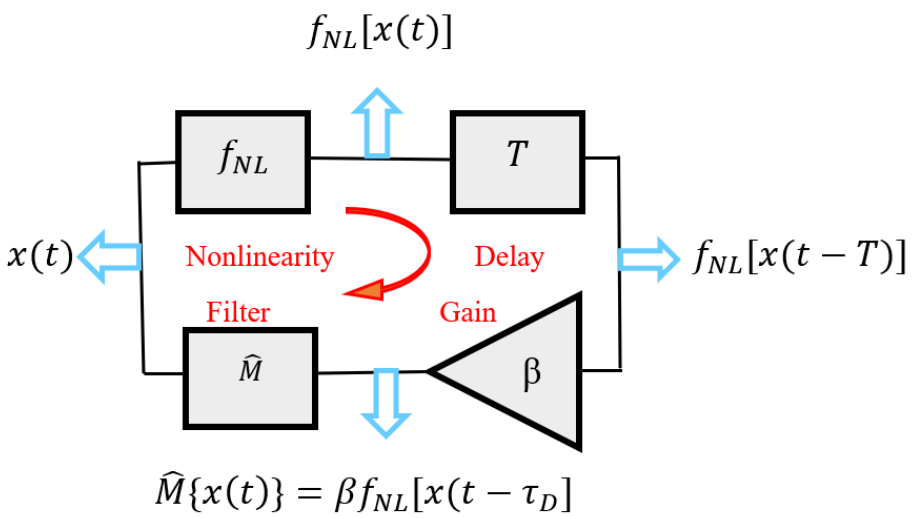

Fig. (1) block diagram of OEO-based Ikeda-like model [6]

2- Model and setup:

In this study, we have modeled MZM using a close loop optoelectronic feedback (OEFB) circuit diagram as an OEO system, which was built as shown in Figure (2) from a symmetric MZM modulator connected to a single mode fiber optic (SMF) of 4 km in length to ensure a 20μs delay time, and the other terminal of the fiber connection with a fast response photodetector (PD) which interned connected to a bandpass filter(BPF). The output signal from the BPF is amplified by an RF amplifier with gain (G), creating a signal called V(t) that includes frequencies in the microwave band and is supplied into the RF-input electrode of the MZM device. With applied voltage V(t), the transmission behavior

of MZM is a nonlinear function, and the transfer function of the OEO is provided by the integro-differential Eq. (1), [7]:

$$x(t) + \tau_H \frac{d}{dt} x(t) + \frac{1}{\tau_L} \int_{t_o}^{t} x(s)ds = \beta cos^2[\, x(t - \tau_D) + \phi] \qquad \ldots. (2)$$

where $x(t) = \frac{\pi}{2} \frac{v(t)}{v_{\pi RF}}$ and $\phi = \frac{\pi}{2} \frac{v_{DC}}{v_{\pi DC}}$ are dimensionless dynamical variable for and phase constant of the system signal respectively. $\beta = \frac{\pi \eta \gamma G S P_i}{2 V_{\pi RF}}$ is the linear gain coefficient, with η which being MZM transmission coefficient, γ is optical fiber transmission coefficient, S is the photodetector sensitivity and P_i is the input power of laser diode LD.

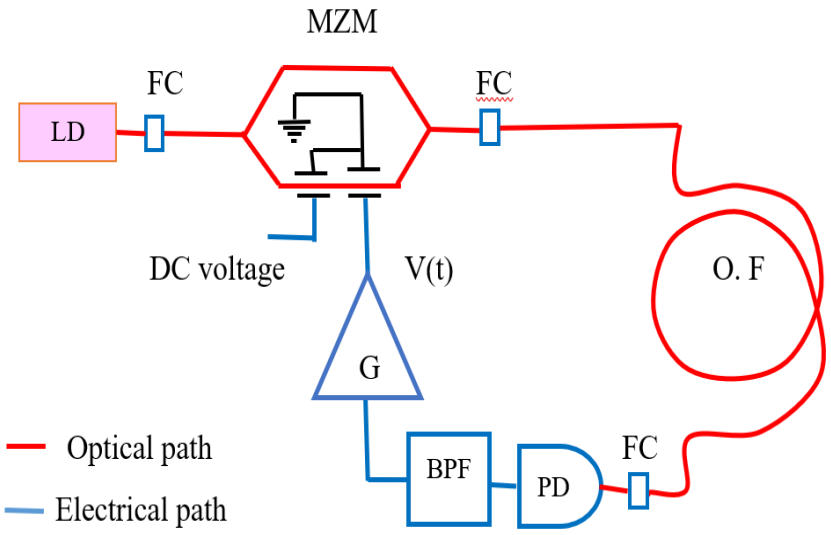

Fig. (2) OEO model with Mach-Zehnder Modulator. The red lines show the optical path and the blue lines show the electrical path. Where:LD: laser diode, FC: fiber convert, MZM: Mach-Zehnder Modulator, FO: Fiber Optic, PD: Photo Detector, G: Gain, BPF: Band Pass Filter, DC: Direct Current, V(t): Input voltage of BPF.

And its half-wave DC and RF voltages are $V_{\pi DC}$ and $v_{\pi RF}$ respectively [8,9]. $\tau_H = \frac{1}{2\pi f_H}$ and $\tau_L = \frac{1}{2\pi f_L}$ are response time constants for high f_H and low f_L cutoff frequencies respectively. τ_D is delay time arising from the optical fiber of length L. introducing new time variable t' in units of time delay τ_D, i.e. $t' = t/\tau_D$, equation (2) can be rewritten as:

$$x(t') + \varepsilon \frac{d}{dt} x(t') + \delta \int_{t_o}^{t'} x(s')ds' = \beta cos^2[\, x(t' - 1) + \phi] \qquad \ldots (3)$$

Where $\varepsilon = \frac{\tau_H}{\tau_D}$ and $\delta = \frac{\tau_D}{\tau_L}$ are new dimensionless parameters. The last equation is dimensionless nonlinear delayed integro-differential equation which refers to slow-fast oscillation dynamics. The last equation Eq. (3) can be solved numerically by delayed differential equation DDE solver package in MATLAB program. For numerical solution purposes, Table (1) contains the main parameter values utilized in the modeling and numerical simulation of the system (3).

Table (1) the main parameters of OEO

Parameter	Value	Unit
Laser diode input power P_i	5	Mw
MZM transmission coefficient	0.8	
MZM splitting ratio (equal)	50% per arm	
MZM DC half wave voltage $V_{\pi DC}$	3.0	Volts
MZM RF half wave voltage $V_{\pi RF}$	3.0	Volts
Optical fiber length L	60-600	m
linear gain coefficient β	3	
Photodetector sensitivity S	1.05	V/Mw
Low pass filter LPF cutoff frequency f_L	22.5	Hz
High pass filter HPF cutoff frequency f_H	0.6	MHz
RF amplifier gain G	3.0	

3- **Results and discussion**

To study the effect of the Time time-delay τ_D on the behavior of a nonlinear system through numerical simulation of the DDE solver program of Eq. (3), all variables havebeen sert fixed as in Table (1), while the value of Time time-delay τ_D changed each time of DDE solver running. Setting time delay τ_D value to 0.3μs and executing the solver MATLAB code, get the Fig.(3a) where the time series of generated RF signals as sinusoidal damped period-one oscillation, this have ensured by its FFT spectrum appear in Fig.(3b), which

refer to single strong frequency, while Fig.(3c) portraits spiral inside loop trajectory plotted by embedding delay technique as X(t) versus X (t- τ_D).

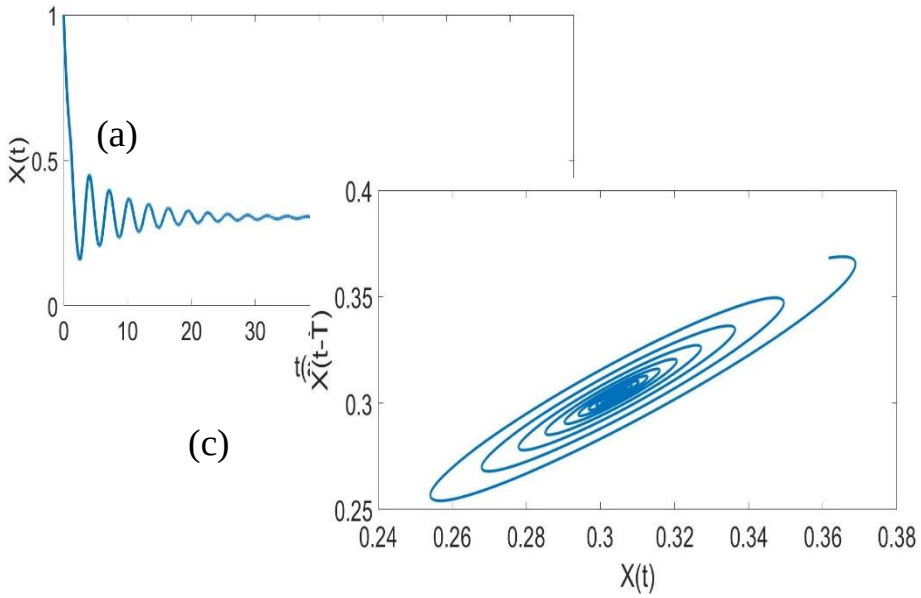

Fig. (3) OEO generated signal τ_D=0.3μs (a) time series of generated signal X(t), (b) FFT frequency spectrum of X(t), (c) phase portrait of X(t).

Increasing the value of time delay τ_D to 0.5μs and simulating Eq. (3) weget the Fig.(3-4a) which appears time series of generated RF-signals X(t) which shows initialized spiky signal that no longer stabilized to period-one oscillation. Fig(3-4b) is the FFT frequency spectrum of X(t) exhibiting high amplitude main frequency component with decreased low amplitudes of frequency harmonics. Fig(3-4c) shows phase diagram trajectory as sharp two edges loop similar to limit cycle trajectory.

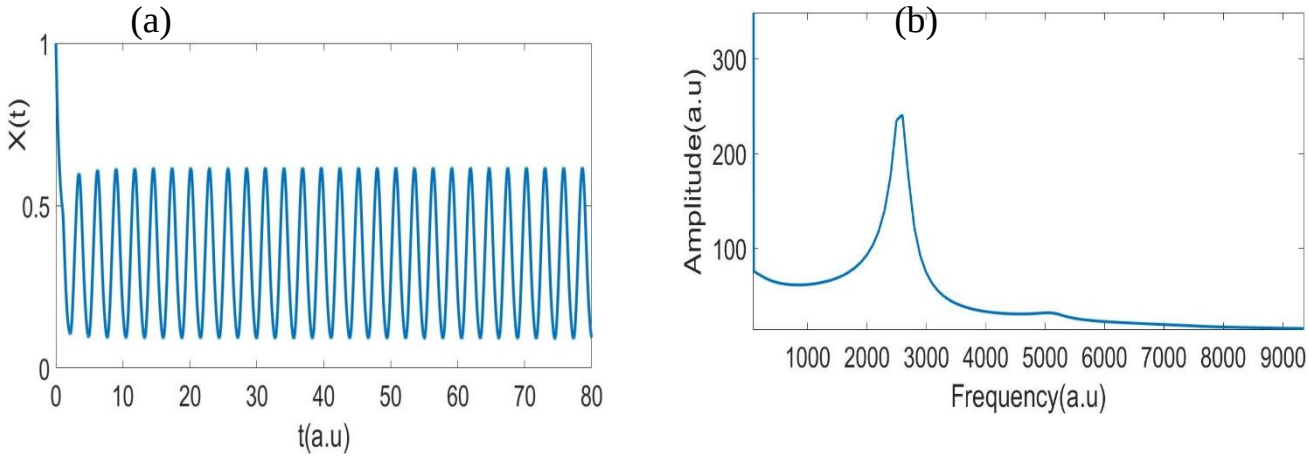

(c)

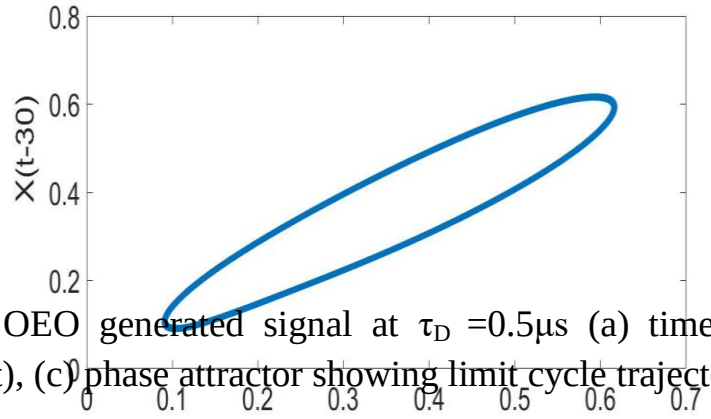

Fig. (4) OEO generated signal at τ_D =0.5μs (a) time series (b) FFT frequency spectrum of X(t), (c) phase attractor showing limit cycle trajectory.

Increasing the value of τ_D to 1.0 μs and enforcement the solver simulation we get the Fig.(3-5a), which shows theoscillation of two different amplitudes referring to occurrence of period doubling oscillation. Fig.(3-5b) is the FFT frequency spectrum that exhibits different exponentially decayed amplitudes, where the main Frequency and the first harmonic have relatively high amplitudes compared to other components, also it could be seen increasing high frequency components indicating emersion fast oscillation with relatively low amplitudes. Fig.(3-5c) portrays phase diagram that shows two overlapped loops the phase trajectory of oscillation with initiation to splitting of some trajectories from the original trajectories, as well as appearing small loops at over right side and lower left side of the main trajectory loops, referring to initiation of fast oscillation with low amplitudes.

(a)

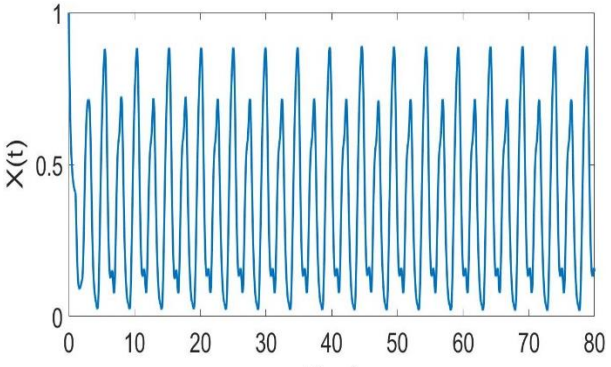

(b)

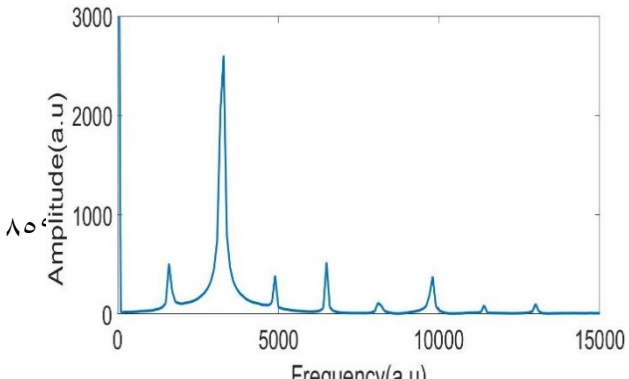

(c)

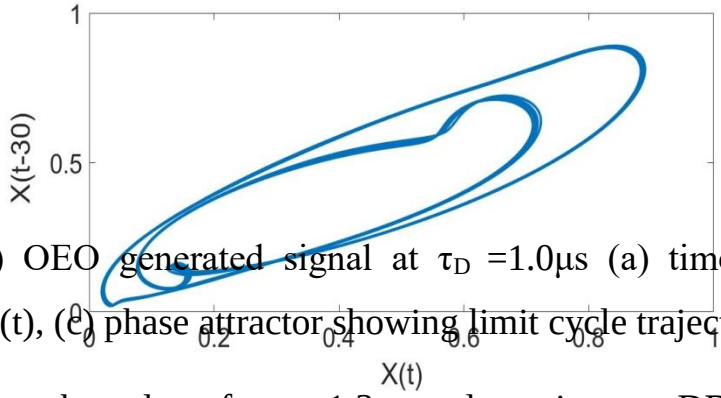

Fig. (5) OEO generated signal at τ_D =1.0μs (a) time series (b) FFT frequency spectrum of X(t), (c) phase attractor showing limit cycle trajectory.

Increasing the value of τ_D to 1.3μs and running our DDE solver, we get the Fig.(3-6a) which shows time series of multi-period oscillation with emerging low amplitudes fast oscillation in-between the slow high-amplitude spikes. Fig(3-6b) appears the FFT spectrum of the oscillation, where the amplitudes of multi-periods appeared. Fig.(3-6c) portrays phase-diagram or the attractor of the oscillation where the multiple wide loops refer to slow oscillations which overlapped with the small narrow loops of fast oscillation, forming mixed-mode oscillation (MMO).

(a)

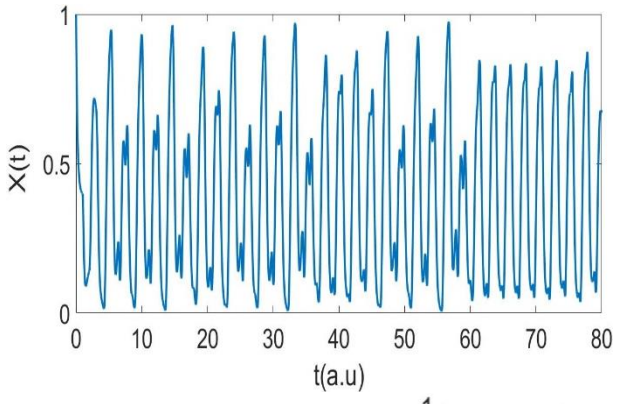

(b)

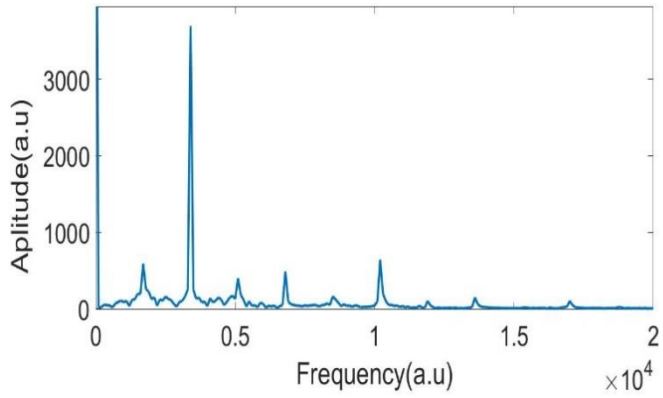

(c)

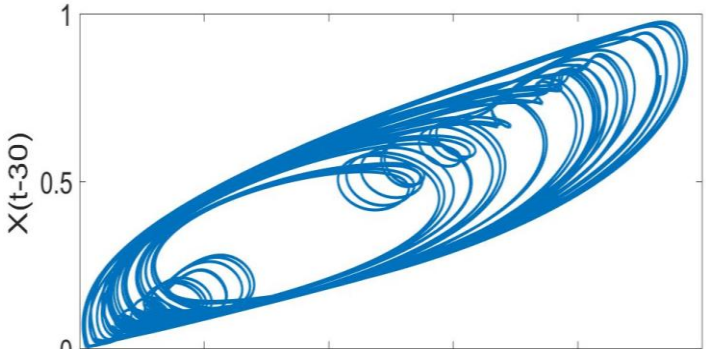

Fig. (6) OEO generated signal at τD =1.3μs (a) time series of multi-period oscillations (b) FFT frequency spectrum of X(t), (c) phase attractor showing limit cycle trajectory.

Setting the value of time delay τD to 1.7μs and executing our DDE solver, we get the Fig.(7a) which explains time series of generated signal X(t) as coexisting different heights amplitudes or spikes, superimposed by low amplitudes fast spikes, forming complex oscillation as quasi-periodic oscillation [10]. Fig.(7b) shows FFT spectrum of generated signal containing different frequency components. Fig.(3-7c) demonstrates overlapped attractor trajectories of different oscillation periods, containing slow wide loops with fast cramped loops, these overlapped trajectories indicate to occurrence quasi-periodic oscillation state of the system.

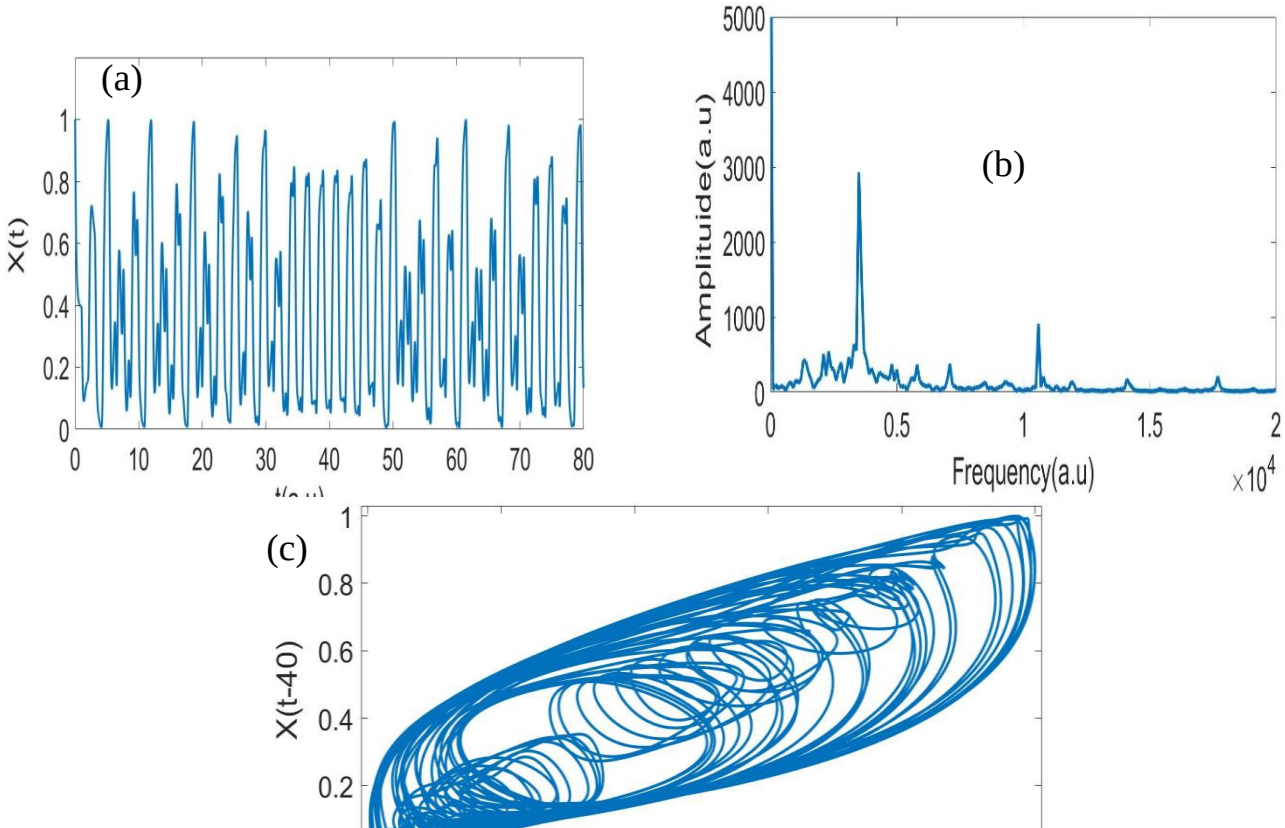

Fig. (7) OEO generated signal at τD =1.7μs (a) time series of quasi-chaotic oscillation (b) FFT frequency spectrum of X(t), (c) phase attractor as multiple wide loops overlapped with other tight loops trajectory.

Increasing the value of delay time τD to 2.5μs and enforcing DDE solver program, we get Fig.(8a) which depicts time series of generated signal X(t), as randomness fluctuation amplitudes indicating to occurrence chaotic oscillation, this where verified by Fig.(8b) which shows FFT frequency spectrum of broadened deferent frequency lines. Fig(8c) portrays attractor diagram of dense overlapped trajectories of multiple randomness oscillations, as chaotic attractor diagram.

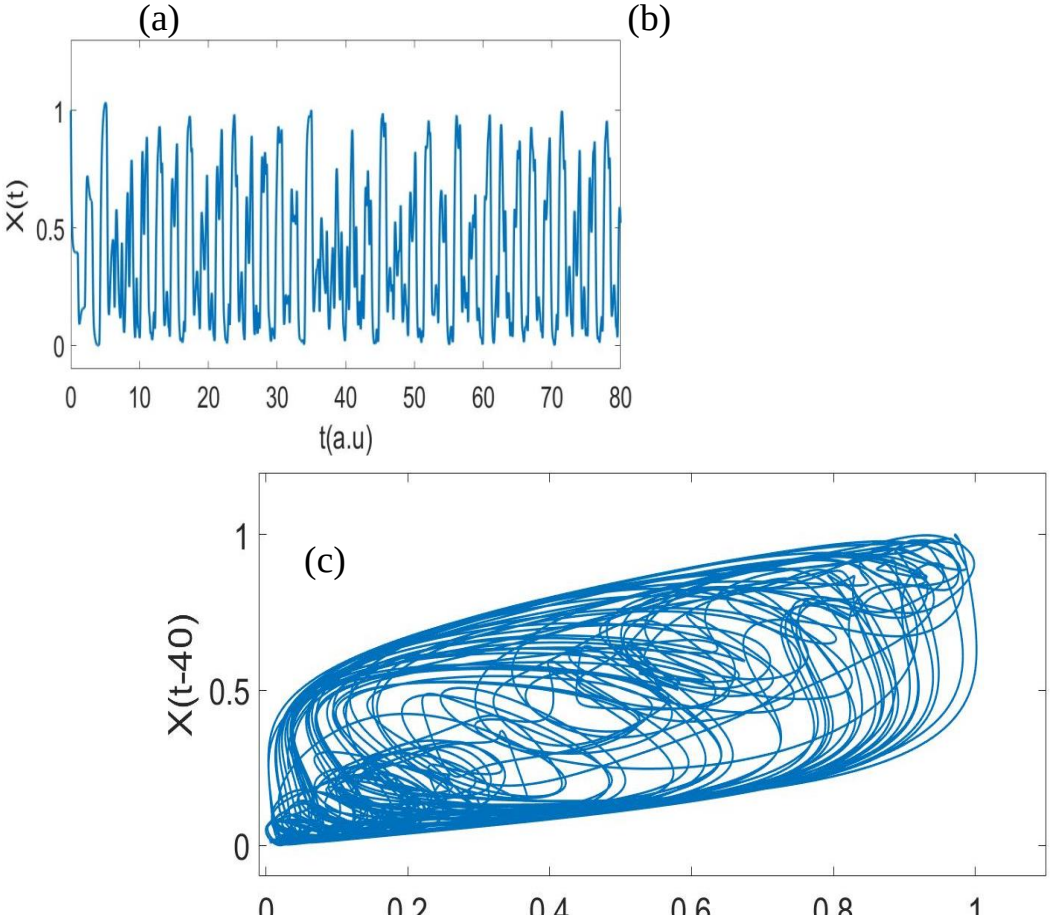

Fig. (8) OEO generated signal at τD =2.5μs (a) time series of quasi-periodic oscillation (b) FFT frequency spectrum of X(t), (c) phase attractor as multiple wide loops overlapped with other tight loops trajectory.

The overall behavior of our OEO system represented by the bifurcation diagram in Fig.(9) which depicts the maximum amplitudes of generated RF oscillation spikes versus control parameter which in this case is the time delay τD of the OEFB; the figure demonstrates different regions of oscillations ranged from single periodic, period doubling, mixed mode, multi-period and chaotic oscillations, depending on the value of delay time τD of OEF.

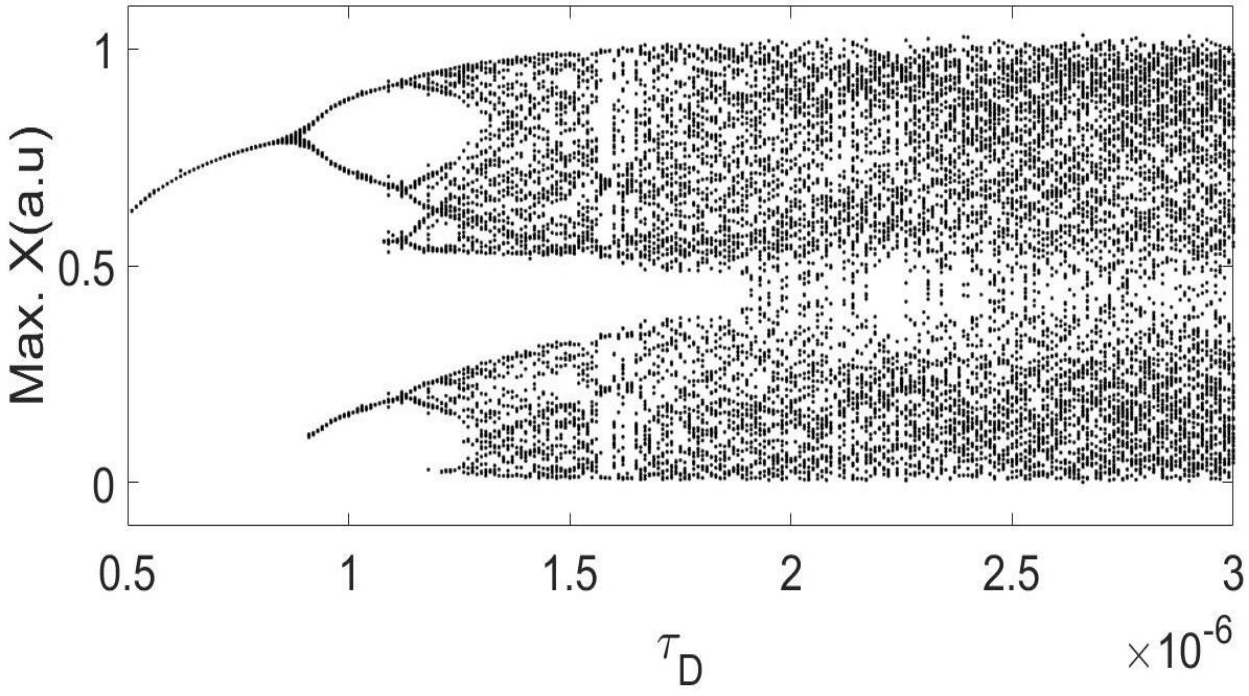

Fig. (9) Bifurcation diagram of maximum values of generated signals X(t) by OEO system as a function of delay time τ_D as a control parameter.

4-Conclusion

Since the time-delay τ_D is a function of different OEO system parameters, hence it could be considered as a control parameter for adjusting dynamical oscillation regimes. The numerical simulation of our OEO model in Eq. (3), showed miscellaneous transitions in dynamic oscillations, starting from period one, period doubling, mixed mode, quasi-periodic and chaotic oscillation, these transitions take place by increasing the value of time-delay τ_D. These dynamical transitions were verified by the bifurcation diagram, which depicts the oscillation path of the OEO system into chaos.

5. Acknowledgements

The authors would like to thank the University of Mosul / Education College for Pure Science for their facilities, which have helped to enhance the quality of this work.

6. References

[1] Salvestrini, P., J., Guilbert, l., Fontana, M., Abarkan, M., and Gille, S.'' Analysis and Control of the DC Drift in LiNbO –Based Mach–Zehnder Modulators''. Hal Open Science, hal-00642162, 2 December 2021.

[2] Velasco-Villa, M., and Rodríguez-Cortés, H.'' Prediction-Based Control for Nonlinear Systems with Input Delay''. Research Article, ID 7415418. October 2017.

[3] Califano, C., and Moog, H.'' Feedback linearization of nonlinear time-delay systems over a time window via discontinuous control''. Hal Open Science, Nov 2021.

[4] Ikeda, K." Multiple-Valued stationary state and its instability of the transmitted light by a ring cavity state". Optics Communications, Volume 30, number 2, August 1979.

[5] Y.K. Chembo, "Laser-based optoelectronic generation of narrowband microwave chaos for radars and radio-communication scrambling", Optics Letters, Vol. 42, No. 17 / September 1 2017.

[6] PENG, H., LEI, P., XIE, X., and CHEN, zh., ‘’ Dynamics and timing-jitter of regenerative RF feedback assisted resonant electro-optic frequency comb’’. Optics Express, Vol. 29, No. 26. 20 Dec 2021.

[7] B. A. Marquez, L. Larger, D. Brunner, Y. K. Chemo, and M. Jacquot, “Interaction between Lienard and Ikeda dynamics in a nonlinear electro-optical oscillator with delayed bandpass feedback”, PHYSICAL REVIEW E 94, 062208 (2016).

[8] Y. C. Kouomou, P. Colet, L. Larger and N. Gastaud, “Chaotic Breathers in Delayed Electro-Optical Systems”, PHYSICAL REVIEW LETTERS, PRL 95, 203903 (2005).

[9] J.P. Goedgebuer, P. Levy, L. Larger, C. C. Chen, and W. T. Rhodes, “Optical Communication with Synchronized Hyperchaos Generated Electro optically”, IEEE JOURNAL OF QUANTUM ELECTRONICS, VOL. 38, NO. 9, SEPTEMBER 2002.

[10] Strogatz, S., H. (2018) ***Nonlinear Dynamics and Chaos.*** Second edition, by Taylor & Francis Group, LLC.P.2.